

# Deep Semantic Graph Matching for Large-scale Outdoor Point Clouds Registration

Shaocong Liu, Tao Wang, Yan Zhang, Ruqin Zhou, Li Li, Chenguang Dai, Yongsheng Zhang, Hanyun Wang

**Abstract**—The current point cloud registration methods are mainly based on geometric information and usually ignore the semantic information in the point clouds. In this paper, we treat the point cloud registration problem as semantic instance matching and registration task, and propose a deep semantic graph matching method for large-scale outdoor point cloud registration. Firstly, the semantic category labels of 3D point clouds are obtained by utilizing large-scale point cloud semantic segmentation network. The adjacent points with the same category labels are then clustered together by using Euclidean clustering algorithm to obtain the semantic instances. Secondly, the semantic adjacency graph is constructed based on the spatial adjacency relation of semantic instances. Three kinds of high-dimensional features including geometric shape features, semantic categorical features and spatial distribution features are learned through graph convolutional network, and enhanced based on attention mechanism. Thirdly, the semantic instance matching problem is modeled as an optimal transport problem, and solved through an optimal matching layer. Finally, according to the matched semantic instances, the geometric transformation matrix between two point clouds is first obtained by SVD algorithm and then refined by ICP algorithm. The experiments are conducted on the KITTI Odometry dataset, and the average relative translation error and average relative rotation error of the proposed method are 6.6cm and 0.229° respectively.

**Index Terms**—Large-scale point clouds; semantic adjacency graph; point clouds registration, optimal transport.

## I. INTRODUCTION

WITH the development of 3D laser scanning technology, point cloud data is widely used in various applications, such as 3D reconstruction, autonomous driving, and smart city construction [1]. As an important research topic, point clouds registration methods are usually adopted to align multiple point clouds obtained from different stations into the same coordinate system.

Currently, point cloud registration methods can be divided into traditional methods and deep learning-based methods. Earlier, the research on traditional point cloud registration methods has made abundant achievements. Stein and Medioni [2] proposed a rough point cloud registration method based

This work was supported in part by the National Natural Science Foundation of China (No. 42271457), a grant from State Key Laboratory of Resources and Environmental Information System, and a grant from the Program of Song Shan Laboratory (Included in the management of Major Science and Technology Program of Henan Province) (No. 221100211000-02). (Corresponding author: Hanyun Wang.)

The authors are with the School of Surveying and Mapping, Information Engineering University, Zhengzhou 450001, China (e-mail: why.scholar@gmail.com).

Color versions of one or more of the figures in this article are available online at <http://ieeexplore.ieee.org>.

on the splash feature descriptor. Besl and McKay [3] proposed the Iterative Closest Point (ICP) algorithm which has been treated as a standard fine registration method for high-precision point cloud registration. Later, many researchers proposed different feature descriptors for point cloud registration, such as Spin Image [4], 3DSC [5], FPFH [6], RoPS [7], B-SHOT [8], BSC [9], KDD [10]. In recent years, with the improvement of computer hardware performance and the rapid development of artificial intelligence, many point cloud registration networks are proposed, for example, DeepVCP [11], DCP [12], PointNetLK [13], PCRNet [14], PREDATOR [15], and GeoTransformer [16]. Because of the large-number of points, the downsampling methods are used to reduce the amount of points and to improve the efficiency of point cloud registration, for example, voxel-grid-based sampling method [17], the Farthest Point Sampling (FPS) method [18], the Inverse Density Importance Sub-Sampling (IDISS) method [19], and the Random Sampling (RS) method. However, the data processed by downsampling strategy is still large, and the extracted points have no special geometric properties. To solve these problems, the keypoints extraction methods are proposed for point clouds registration, and can be divided into hand-crafted detectors and deep learning-based detectors. Hand-crafted detectors extract keypoints with significant geometric features through specific rules, for example, Intrinsic Shape Signatures (ISS) [20], Key Point Quality (KPQ) [21] and Harris 3D [22]. Affected by the changes of the scanning angles and occlusions between objects in the scenes, keypoints with the same geometric features are not necessarily repeatable. The deep learning-based detectors extract repeatable and stable keypoints through data-driven manner, and achieve better point cloud registration performance, for example, Kpsnet [23], PRNet [24], DeepVCP [11] and D3Feat [25]. Liu et al. [26] rethought four keypoints detectors and compared their performance, and the experiments showed that the MLP-Detector is the best keypoints detector on large-scale outdoor scenes. However, all of the above methods are based on the geometric features of point clouds, and completely ignore the semantic information in the point cloud registration task.

Semantic information has shown impressive effectiveness for many point cloud research tasks, for example, scene recognition [27], closed-loop detection [28], and point cloud registration [29]. At present, the point cloud registration work using the semantic information is few, and the semantic information is only limited to the classification of point cloud. Li et al. [29] firstly divided the point cloud into different subsets based on semantic labels, and then used the ISS and FPFH

method to extract the keypoints and calculate the features

of each keypoint, and finally utilized the RANSAC to reject incorrect correspondence and calculate the transformation matrix. However, this approach has the following disadvantages. First, the performance of the registration relies heavily on the result of point cloud segmentation. Secondly, the semantic information is only used for segmentation and not used for the downstream point cloud registration task.

In order to explore the effectiveness of semantic information for point cloud registration, we treat the point cloud registration problem as a semantic instances matching and registration task, and propose a deep semantic graph matching network for large-scale point cloud registration. Firstly, we obtain semantic labels of the large-scale outdoor point cloud by semantic segmentation network and merge the neighboring point clouds with the same semantic labels by clustering algorithms to acquire the spatial location of semantic instances, and carry out One-Hot encoding method to obtain the semantic information. Secondly, we construct a semantic adjacency graph based on the spatial adjacency relationship of semantic instances and obtain the high-dimensional features of spatial location and semantic information by graph convolutional network (GCN), and we extract the high-dimensional features of the geometric shape through the PointNet, and then we utilize the attentional mechanism module to enhance the features. Then, we convert the semantic instances matching problem to the optimal transmission problem, and the corresponding relationships between semantic instances are calculated refer to the Superglue method. Finally, according to the correspondence between semantic instances, the transformation matrix between two point clouds are obtained by SVD (singular value decomposition) and ICP algorithm.

To the best of our knowledge, we are the first to use the semantic instances as the processing units for point clouds registration. In summary, our contributions can be summarized as follows:

- 1) This paper models the large-scale point cloud registration problem as semantic instances matching and registration problem, and proposes a deep semantic graph matching network for point clouds registration.
- 2) This paper presents a method of semantic instance feature extraction. We use GCN to extract spatial location, semantic categorical features and utilize MLP to extract geometric shape features, and then concatenate them as the features of each instance.
- 3) This paper carries out the semantic instances matching and large-scale point cloud registration experiments on KITTI Odometry dataset, and the results demonstrate that our method achieves high accuracy of both the semantic instances matching and point clouds registration.

## II. RELATED WORK

The task of point cloud registration is to calculate a rigid matrix including rotation matrix and translation vector, and then uses this rigid matrix to transform the source point cloud to the target point cloud. Point cloud registration methods can be divided into traditional methods and deep learning-based methods. Traditional point cloud registration methods

include ICP [3], RANSAC [30], 4PCS algorithm [31], Super 4PCS algorithm [32] and so on. The traditional point cloud registration methods are low-hardware requirements, easy to implement, strongly interpretable, and do not require time-consuming training process. However, the traditional methods are easy to fall into local minima, and are affected by the operators' experience and parameter adjustment ability to match the correspondences by hand-craft features. In addition, coarse registration methods are often time-consuming and not suitable for some real-time applications. With the development of computer hardware and the progress of artificial intelligence technology, deep learning-based point cloud registration methods have been studied in recent years. In this section, we will give a brief overview of the progresses of deep learning-based point cloud registration methods and deep graph matching methods.

### A. Deep Learning-based Point Cloud Registration

**Registration based on global features:** PointnetLK [13] uses PointNet [33] and max pooling operation to extract global features of point cloud, and then iteratively estimates transformation parameters by improved Lucas Kanade (LK) algorithm. PCRNet [14] concatenates two global features obtained by PointNet and feeds them into multilayer perceptron (MLP) to estimate the rotation quaternion and three translation parameters directly. CorsNet [34] uses the global features for correspondence estimation, and finally uses SVD to calculate the transformation matrix. OMNet [35] concatenates the global features extracted from the source and target point clouds by using MLP and max pooling operation, and then obtains the transformation matrix through rigid transformation regression network. SCANet [36] uses the fully connected layer, spatial attention module and max pooling layer to obtain the global features of each point, and then uses the channel cross-attention module and the fully connection layer to revert the global features to the seven transformation parameters. It is efficient to use global features for point cloud registration, however, these methods need high accuracy of learned feature and the appropriate designment for the depth and width of regression network.

**Registration based on keypoint detector:** PRNet [24] utilizes the saliency scores calculated by the L2 norm of features to obtain the keypoints, which are then matched as corresponding points for point cloud registration. Kpsnet [23] takes the keypoints with high saliency scores as candidate points, and establishes the correspondence through the alignment module for point cloud registration. USIP network utilizes the keypoints with the smallest salient uncertainties computed by the FPN (Feature Proposal Network) to construct corresponding point pairs. D3Feat [25] treats points with maximal scores across the spatial and channel dimensions as the 3D keypoints, and the correspondences obtained through nearest neighbors finding in the feature space are used to calculate the transformation matrix. 3D3L [37] takes points as the keypoints with larger values in the score map. Liu et al. [26] evaluated four kinds of keypoint detectors based on D3Feat network, and found that the MLP-Detector obtains the best keypoint

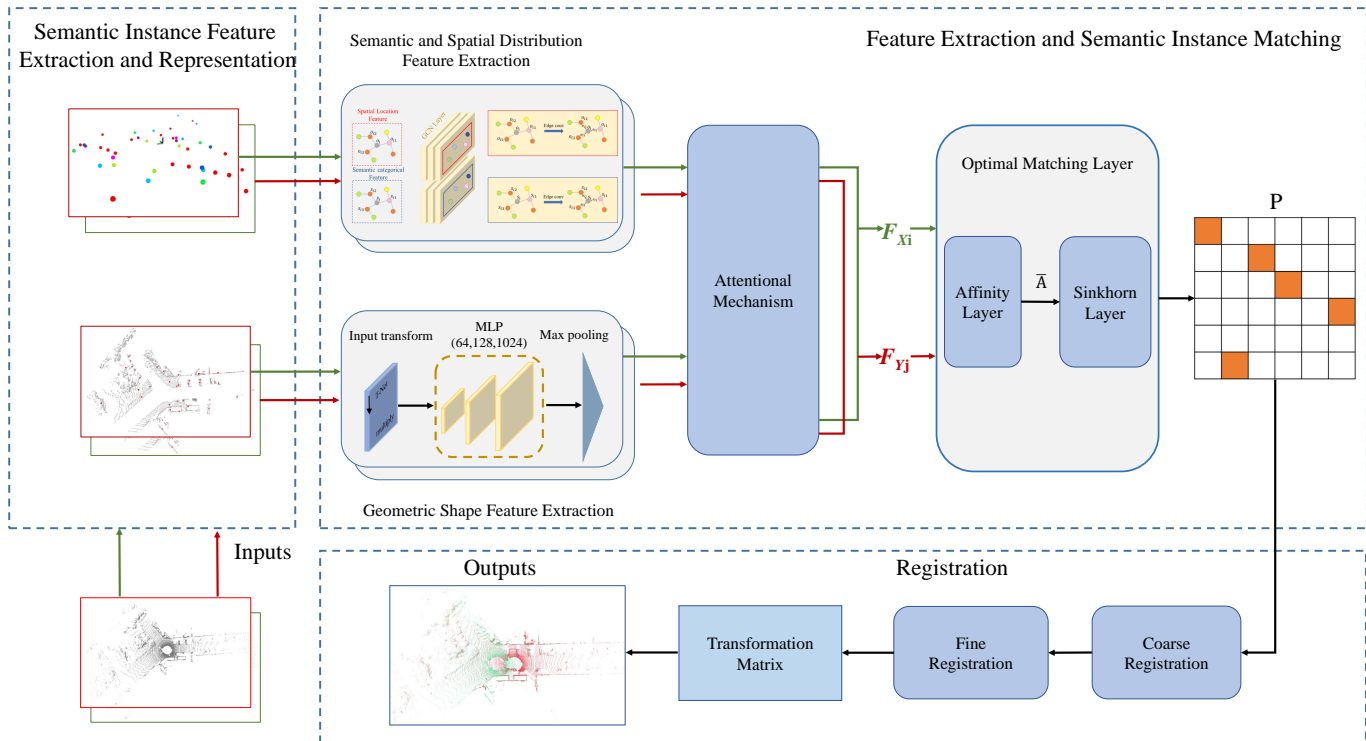


Fig. 1: The overall pipeline of the proposed method.

detection and point cloud registration performance on the large-scale datasets.

**Registration based on semantic information:** The research for point cloud registration based on semantic information is relative rare compared with other kinds of methods. Li et al. [29] first used semantic information in source and target point clouds for segmentation, and then extracted the keypoints and calculated the correspondences by intrinsic shape signatures (ISS) [20] and Fast Point Feature Histograms (FPFH) [6] respectively. Finally, the transformation matrix with the highest accuracy obtained from different category objects is selected as the final transformation matrix.

### B. Deep Graph Matching













Graph matching has been discussed in pattern recognition and computer vision for decades [38]–[41]. In recent years, research on deep learning-based graph matching has attracted more and more attentions. To preserve the global and local structures of the graph, Nie et al. [42] proposed the hyper-clique graph (HCG) matching method by replacing the nodes and hyper-edges with cliques (a set of neighboring nodes in a specific feature space) and hyper-edge linking multiple cliques. Zhang et al. [43] proposed two effective optimized algorithms to solve the second- and high-order graph matching problems. (1) For the second-order graph matching, a K-nearest-neighbor-pooling matching method was proposed to integrate feature pooling into graph matching. (2) For the high-order graph matching, a sub-pattern structure was introduced for the robust graph matching method. Andrei and Cristian [44] extracted the first-order and second-order features of the graph

structure to construct the similarity matrix, and obtained the matching results according to the graph matching algorithm. Wang et al. [45] proposed an end-to-end deep network pipeline for graph matching by embedding edge information into node feature space.

## III. METHODOLOGY

In this paper, to explore the effectiveness of semantic information for point cloud registration, we treat the point cloud registration problem as a semantic instances matching and registration task, and propose a deep semantic graph matching network for large-scale point cloud registration. The overall pipeline of the proposed method is shown in Fig. 1. The proposed network consists of three main parts: semantic instance extraction and representation, feature extraction and semantic instance matching, and point clouds registration. The semantic instance extraction and representation module takes the original point cloud data as input and uses semantic segmentation network to extract the semantic instance. The feature extraction and semantic instance matching module first constructs the graph based on the semantic instances and their spatial neighboring instances, and then learns the spatial location features and semantic categorical features through graph convolutional network (GCN), and finally learns geometric shape features through the PointNet module for each node. The learned features are then augmented through self-attention layer and cross-attention layer, and the semantic instance matching is conducted through optimal matching layer. The point cloud registration module takes matched semantic instances as inputs, and utilizes the coarse and fine

TABLE I: The colors of 12 classes of semantic instances.

Num	Color	Class	Num	Color	Class
0		Car	6		Fence
1		Truck	7		Vegetation
2		Other Vehicle	8		Trunk
3		Sidewalk	9		Terrain
4		Other Ground	10		Pole
5		Building	11		Traffic Sign

registration strategy sequentially to estimate the transformation matrix.

### A. Semantic Instances Extraction and Representation Module

Inspired by the work [27], we think that humans find out the same object from two scenes through semantic information and their topological relations. To explore the effectiveness of semantic information for point cloud registration, we take the semantic instances as the basic processing units to replace the points in the original point clouds. Compared with conventional methods directly processing 3D points, semantic instances are more distinguishable and can also greatly reduce the computational burden.

Given an original point cloud denoted as  $P = \{p_1, p_2, \dots, p_m | p_i \in R^3\}$ , we first use RangeNet++ [57] to conduct semantic segmentation on point clouds (N clusters of semantic instances are obtained by using Euclidean clustering with different radii for different classes of objects, which are denoted as  $C = \{C_1, C_2, \dots, C_N\}$ ,  $C_i = \{p_1, p_2, \dots, p_r | p_i \in R^3\}$ , and obtain semantic categorical label for each point in the point clouds. Then, spatial clustering algorithm is applied to extract semantic instances (we calculate the centroid of each cluster point cloud to obtain the spatial location of instances, and encode the semantic categorical information with one-hot vector according to the categorical label, which denoted as  $o_i = (x_{I_i}, y_{I_i}, z_{I_i})^T$  and  $s_i = (s_i^1, s_i^2, \dots, s_i^{12})^T$  and classes with a small number of points (for example, person) are ignored during this process. In addition, in order to obtain the geometric shape information of each instance, we use the farthest point sampling method to obtain k points from original point cloud belonging to each instance, which is denoted as  $p_i = \{p_{i1}, p_{i2}, \dots, p_{ik} | p_{ik} \in R^3\}$ . Finally, the semantic instances contain three kinds of attributes, including the spatial location information, semantic category information and global shape information, which are denoted as  $I_i = \{o_i, s_i, p_i\}$ .

Table I lists the final 12 classes of semantic instances of KITTI Odometry dataset used in this paper. Fig. 2 visualizes the extracted semantic instances of two scenes and different colors represent different semantic classes.

### B. Feature Learning Module

**Semantic instance adjacency graph construction.** In order to fully describe the spatial location and topological relationship of semantic instances, we construct the semantic instance adjacency graph by using the location of semantic instances (shown as Fig. 3). First, the semantic instances of

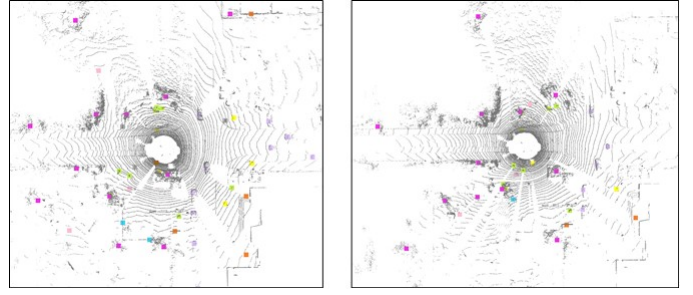


Fig. 2: The semantic instances extracted from two scenes.

two large-scale point clouds are taken as the graph nodes, and represented as  $I_X = \{I_1, I_2, \dots, I_m\}$  and  $I_Y = \{I_1, I_2, \dots, I_n\}$  respectively. Secondly, the edges  $E_X$  and  $E_Y$  of two graphs are constructed by selecting k closet semantic instances for each semantic instance according to the location information. Two semantic adjacency graphs are finally represented as  $G_X = \{I_X, E_X\}$  and  $G_Y = \{I_Y, E_Y\}$  respectively.

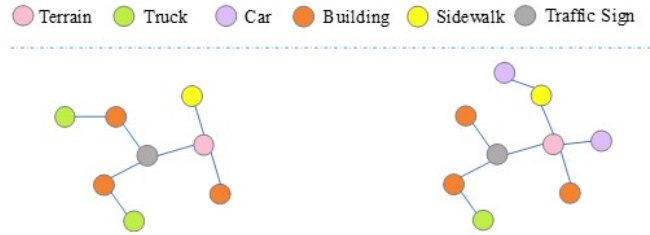


Fig. 3: Semantic instance adjacency graph based on spatial location.

**Semantic and spatial location feature learning.** Inspired by the DGCNN [46], in this section, we take the EdgeConv as the core layer, and design a three-layer graph convolutional neural network to learn semantic categorical features and spatial location features, as shown in Fig. 4.

As described in Section III-A, each semantic instance contains spatial location information  $o_i = (x_{I_i}, y_{I_i}, z_{I_i})^T$  and semantic categorical information  $s_i = (s_i^1, s_i^2, \dots, s_i^{12})^T$  represented by one-hot encoding vector. Since these two attributes describe different characteristics of semantic instances, we use the graph convolutional neural network to extract the features of these two attributes respectively. For the semantic instance  $I_i$  with spatial location feature  $o_i = (x_{I_i}, y_{I_i}, z_{I_i})^T$  and semantic categorical information  $s_i = (s_i^1, s_i^2, \dots, s_i^{12})^T$ ,  $k$  neighborhood semantic instances  $I_{ineigh} = \{I_{i1}, I_{i2}, \dots, I_{ik}\}$  are first selected according to the edges in the semantic adjacency graph, and the corresponding  $k$  spatial location features and semantic categorical features are represented by  $o_{ineigh} = (o_{i1}, o_{i2}, \dots, o_{ik})^T$  and  $s_{ineigh} = (s_{i1}, s_{i2}, \dots, s_{ik})^T$  respectively. Then, the graph convolutional neural network is used to learn the spatial location features and semantic categorical features. Assuming that the input features to the  $l$ -th layer is  $o_i^{(l)}$ , the output feature of the  $l$ -th layer can be formulated as follows:

$$o_i^{(l+1)} = \sum_{o_j^{(l)} \in o_{ineigh}^{(l)}} \varphi_i(o_i^{(l)}, o_j^{(l)} - o_j^{(l)}) \quad (1)$$

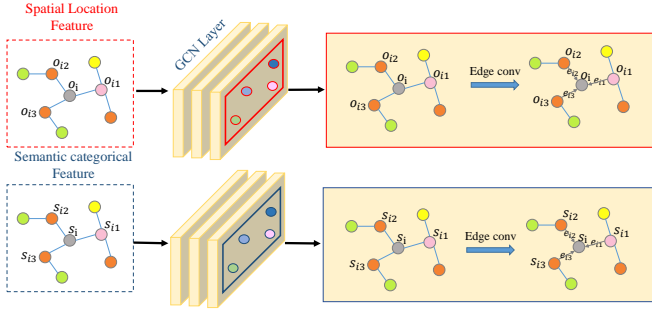


Fig. 4: Graph convolutional network in our method.

$$s_i^{(l+1)} = \sum_{s_j^{(l)} \in s_{i \text{ neighbor}}^{(l)}} \bar{\varphi}_i(s_i^{(l)}, s_i^{(l)} - s_j^{(l)}) \quad (2)$$

where,  $\varphi_i$  and  $\bar{\varphi}_i$  represent the weight parameters respectively.

According to the topological relationship between the semantic instance and its neighborhood semantic instances, we finally obtain two high-dimensional features  $o_i^{(3)}$  and  $s_i^{(3)}$  of each semantic instance by graph convolutional neural network.

**Geometric shape feature learning.** After data processing described in Section 3.1, the maximum number of semantic instances in one scene is less than 100 (including semantic instances that cannot be used due to changes in perspective or object occlusion), which results in less information obtained from these semantic instances. Therefore, we consider using geometric shape features of semantic instances to enhance the learned features. For semantic instance  $I_i$ , we extract  $k$  points belonging to the instances according to the farthest distance sampling strategy, which are represented as  $p_i = \{p_{i1}, p_{i2}, \dots, p_{ik} | p_{ik} \in R^3\}$ . Then, we utilize the PointNet to extract global shape features, as shown in the Fig. 5.

Firstly, the T-Net is trained to normalize the features of the input point cloud. For  $k$  points (denoted as  $p_i = \{p_{i1}, p_{i2}, \dots, p_{ik} | p_{ik} \in R^3\}$ ) selected from semantic instance  $I_i$ , we utilize the multi-layer perceptron (MLP) to estimate 9 parameters of transformation matrix  $H$ , and transform the points belonging to the semantic instance according to  $H$ , which is formulated as follows:

$$\tilde{P}_i^T = H P_i^T \quad (3)$$

Secondly, the MLP layer, consisting of the fully connected layer, batch normalization function and ReLU activation function, is used for feature extraction, as shown in Fig.5. The feature extraction process based on MLP can be formulated as follows:

$$h_i^{(l)} = R(\phi^{(l)}(W^{(l)} \tilde{P}_i^{(l)} + b^{(l)})) \quad (4)$$

where  $l = 1, 2, 3$  represents the index of layers of the MLP,  $\phi$  represents the batch normalization function, and  $R$  represents the ReLU activation function. Finally, we use the maximum pooling layer to obtain the geometry shape feature  $h_i$  for the semantic instance  $I_i$ .

**Attentional mechanism.** As described before, spatial location features and semantic categorical features of semantic

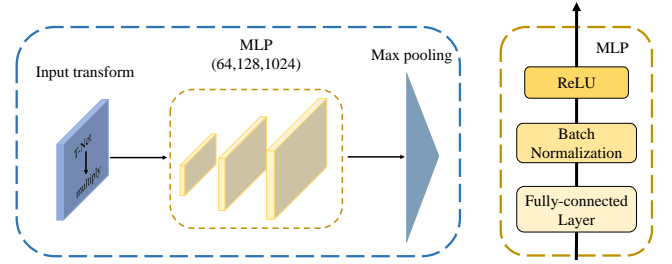


Fig. 5: the geometrical shape feature extraction network.

instances are extracted from  $k$  nearest neighbor semantic instances, and the geometric shape features are extracted from the points belonging to the semantic instances themselves. To further promote the feature discrimination ability, we propose a feature enhancement method based on attention mechanism. Specifically, the self-attention mechanism is utilized to effectively capture the context information from all semantic instances in a single scene, and the cross-attention mechanism is utilized to effectively capture the context information from the semantic instances cross different scenes. The schemas of self-attention mechanism and cross-attention mechanism are shown in Fig. 6: We take the spatial location features as an example to introduce the feature enhancement process based on self-attention mechanism and cross-attention mechanism. Firstly, for semantic instances  $I_i \in I_X$  and  $I_j \in I_X$  in the same scene, we calculate their  $q_i$ ,  $k_i$  and  $v_i$  respectively by using the self-attention mechanism according to their high-dimensional features  $o_i^{(3)}$  and  $o_j^{(3)}$ . The detailed functions are described as follows:

$$q_i = W_1 o_i^{(3)} + b_1 \quad (5)$$

$$\begin{bmatrix} k_j \\ v_j \end{bmatrix} = \begin{bmatrix} W_2 \\ W_3 \end{bmatrix} o_j^{(3)} + \begin{bmatrix} b_2 \\ b_3 \end{bmatrix} \quad (6)$$

where parameters  $W$  and  $b$  are shared in the same scene for all semantic instances.

Then, we calculate the weight score  $\alpha_{ij}^{self}$  of the spatial location features between semantic instance  $I_i$  and  $I_j$ , and the formula is expressed as follows:

$$\alpha_{ij}^{self} = \text{softmax}(q_i^T k_j) \quad (7)$$

Finally, the spatial location feature  $o_i^{self}$  of semantic instance  $I_i$  after self-attention mechanism can be obtained by weighted summation of features of all other semantic instances. The calculation formula is as follows:

$$o_i^{self} = \sum_{j=1}^m \alpha_{ij}^{self} o_j^{(3)} \quad (8)$$

For any semantic instance  $I_i$ , the cross-attention mechanism is to calculate the attention scores of features between  $I_i$  and semantic instances from another scene, and then the final feature is obtained by weighted summation of features from another scene. Firstly, for semantic instances  $I_i \in I_X$  and

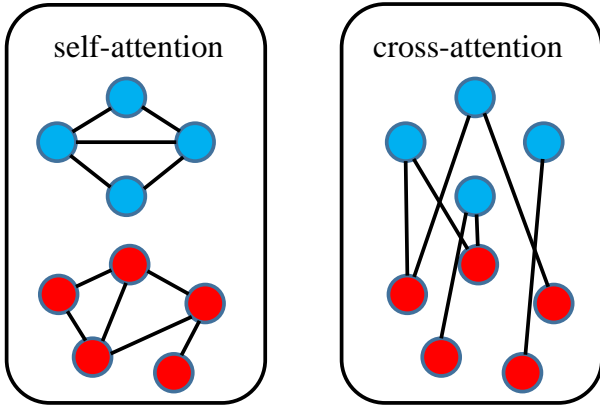


Fig. 6: The schemas of self-attention mechanism and cross-attention mechanism.

$I_j \in I_Y$  in different scenes, we calculate the  $q_i$ ,  $k_i$  and  $v_i$  according to their spatial location features  $o_i^{self}$  and  $o_i^{self}$ , and the formulas are expressed as follows:

$$q_i = W_4 o_i^{self} + b_4 \quad (9)$$

$$\begin{bmatrix} k_j \\ v_j \end{bmatrix} = \begin{bmatrix} W_5 \\ W_6 \end{bmatrix} o_j^{self} + \begin{bmatrix} b_5 \\ b_6 \end{bmatrix} \quad (10)$$

Then, we calculate the weight score  $\alpha_{ij}^{cross}$  of the spatial location features between semantic instances  $I_j$  and  $I_i$ , and obtain the spatial location features by weighted summation of features of all semantic instances from another scene according to  $\alpha_{ij}^{cross}$ . The formulas are expressed as follows:

$$\alpha_{ij}^{cross} = \text{softmax}(q_i^T k_j) \quad (11)$$

$$o_i^{cross} = \sum_{j=1}^m \alpha_{ij}^{cross} o_j^{self} \quad (12)$$

In attention mechanism, the enhancement process of semantic categorical feature  $s$  and geometric shape feature  $h$  is similar to spatial location feature  $f$ . After enhancement by self-attention mechanism and cross-attention mechanism, the high-dimensional features of semantic instance  $I_i$  are represented by  $o_i^{cross}$ ,  $s_i^{cross}$  and  $h_i^{cross}$  respectively. Finally, the feature  $F_i$  of semantic instance is obtained by concatenating the  $o_i^{cross}$ ,  $s_i^{cross}$  and  $h_i^{cross}$ , and is formulated as follows:

$$F_i = \text{concat}(o_i^{cross}, s_i^{cross}, h_i^{cross}) \quad (13)$$

### C. Optimal Matching Layer

At present, the optimal transport model has been widely used in keypoint matching and domain adaption fields. It is to obtain a mapping minimizing the cost of mapping from one distribution to another. Based on the advantage of obtaining the minimum global matching cost of the optimal transport model, we use it to implement the semantic instance matching. Firstly, for feature  $F_{I_X}$  of semantic instance set  $I_X$  and feature

---

### Algorithm 1 Sinkhorn algorithm.

---

**Inputs:** similarity matrix  $\bar{A}$ , and number of iterations  $I$

**Outputs:** soft assignment matrix  $\bar{A}$

**Initialization:**  $\bar{A}^{(0)} = \bar{A}$ ,  $k = 1$

**while**  $k < I$  **do**  
 $\bar{A}^{(k)'} = \bar{A}^{(k-1)} \oslash (\bar{A}^{(k-1)} L_M)$   
 $\bar{A}^{(k)} = \bar{A}^{(k)'} \oslash (L_N \bar{A}^{(k)'})$   
 $k = k + 1$   
**end while**  
 $\bar{P} = \bar{A}^{(k)}$

---

$F_{I_Y}$  of semantic instance set  $I_Y$ , affinity matrix  $A \in M \times N$  is obtained to predict the similarity matrix according to  $F_{I_X}$  and  $F_{I_Y}$ , and is formulated as follows:

$$A = (F_{I_X})^T W (F_{I_Y}) \quad (14)$$

where  $W$  is the parameter optimized by the neural network. Through the affinity matrix  $A$ , the element  $A_{ij}$  between any semantic instances  $I_i \in I_X$  and  $I_j \in I_Y$  can be obtained. Compared with the similarity obtained by directly calculating the inner product of two semantic instance features, the affinity matrix obtained through optimal transport layer is optimized in a global manner. Secondly, because not all semantic instances in one scene have counterpart in another scene, similar to Superglue, we add a row and a column to the end of the affinity matrix, and is formulated as follows:

$$\bar{A}_{i,N+1} = \bar{A}_{M+1,j} = \bar{A}_{M+1,N+1} = z \in R \quad (15)$$

The row  $M + 1$  and column  $N + 1$  of similarity matrix  $\bar{A}$  are called dustbin. Through this manner, semantic instances without corresponding instances are put into dustbin.

Then, we use the Sinkhorn algorithm to solve the optimal transport problem, and obtain the soft assignment matrix. Sinkhorn algorithm is a differentiable Hungarian algorithm which normalizes the affinity matrix  $\bar{A}$  along rows and columns iteratively. The algorithm of Sinkhorn is shown in Algorithm 1, where  $\oslash$  represents element-by-element division, and  $L_M \in M \times M$  and  $L_N \in N \times N$  are identity matrices.

Finally, the semantic instance in  $A$  will be assigned to a single semantic instance in  $B$  or the dustbin. After removing the  $M + 1$  row and  $N + 1$  column of the matrix  $\bar{P}$ , the remaining matrix  $P$  is the soft assignment matrix of two semantic instance sets from two scenes.

### D. Loss Functions

To make the obtained semantic instance matches close to the ground truth matches  $\Theta = \{(i, j)\}_t \subset I_X \times I_Y$ , we minimize the negative log-likelihood  $P_{ij}$ , and is formulated as follows:

$$\text{Loss} = - \sum_{(i,j) \in \Theta} \log P_{ij} \quad (16)$$

According to the soft assignment matrix  $P$ , we can obtain two corresponding semantic instance sets  $\Phi \subset I_X \times I_Y$  and it should meet the following conditions:

TABLE II: The inlier ratios on the KITTI Odometry.

Method	Points	Inlier Ratio (%)
LM-Detector	250	15.97
$L_2$ -Detector	250	9.66
FDN-Detector	250	15.85
MLP-Detector	250	46.59
ours	<250	<b>54.25</b>

$$\forall (I_{X_i}, I_{Y_j}) \in \Phi, P_{ij} > T \quad (17)$$

where  $P_{ij}$  is the score of matching semantic instances  $I_{X_i}$  and  $I_{Y_j}$  in the soft assignment matrix  $P$ , and  $T = 0.65$  is a predefined probability threshold.

### E. Registration Based on Matched Semantic Instances

After obtaining the matched semantic instances of two point clouds, a coarse-to-fine registration strategy is used to align two point clouds.

**Coarse registration.** According to the matched semantic instance set  $\Phi$  and corresponding spatial location  $O$  of two point clouds obtained in Section III-A, we utilize the singular value decomposition (SVD) method to estimate the geometric transformation between two point clouds. Influenced by the factors such as occlusions and variations of scanning distances during point cloud acquisition, the spatial locations of the semantic instances in the two point clouds cannot accurately represent the real locations of the ground objects. Therefore, the geometric transformation matrix calculated according to the spatial locations of the matched semantic instances can only be used for coarse registration between two point clouds.

**Fine registration.** Based on the geometric transformation matrix  $\{R_c, T_c\}$  obtained by the SVD algorithm, we adopt the ICP algorithm to further optimize the transformation matrix. Specifically, we put the KITTI Odometry data as the original point cloud to be registered, then utilize the ICP algorithm iteratively to obtain the final transformation matrix  $\{R, T\}$ , which minimizes the error function  $E(R, T)$  of source point cloud P and target point cloud Q.

## IV. EXPERIMENTS

### A. Implementation Details

The framework of our experiments is based on Pytorch 1.12 and Ubuntu 20.04, and all experiments are conducted on workstations with an Intel Core i9-9700 CPU, 16GB RAM, and 24GB NVIDIA Titan GPU. The performances of our proposed methods are tested on large-scale outdoor point cloud KITTI Odometry dataset. To learn the global shape feature for each semantic instance, 128 points belonging to each semantic instance are selected based on FPS algorithm. In the semantic graph construction stage, the number of neighboring semantic instances is set to 10, and the output feature dimensions extracted by the graph convolutional neural network are set to 64, 64, and 128 respectively. For the optimal matching layer, we set the distance threshold as 0.7. The batch size, the initial parameters of momentum optimizer, and weight decay are set to 32, 0.0001, and 0.98 respectively.

TABLE III: Registration performance on KITTI Odometry.

Methods	RTE		RRE	
	AVG	STD	AVG	STD
3DFeatNet	25.9	26.2	0.57	0.46
SKD+3DFeatNet	14.0	13.4	0.57	0.48
FCGF	9.52	1.3	0.3	0.28
D3Feat	6.9	0.3	0.24	<b>0.06</b>
Ours	<b>6.13</b>	<b>0.08</b>	<b>0.22</b>	0.27

### B. Testing Dataset and Evaluation Metrics

**Testing dataset.** The KITTI Odometry dataset contains the large-scale outdoor point clouds obtained by Velodyne HDL64 and ground-truth POS provided by GPS/INS system. In our method, the training set contains 9578 point clouds from 0-5 sequences, the validation set contains 1907 point clouds from 6-7 sequences, and the test set contains 440 point clouds from 8-10 sequences.

**Evaluation metrics.** Four evaluation metrics including inlier ratio, instance matching accuracy, relative translation error (RTE) and relative rotation error (RRE) are adopted in this section. The inlier ratio  $I$  is calculated by the following formula:

$$I = \frac{1}{|\Psi|} \sum_{(o_{x_i}, o_{y_j}) \in \Omega} 1 (\| (R_T o_{x_i} + T_T) - o_{y_j} \| < \beta) \quad (18)$$

where  $\Psi$  and  $\Omega$  are the spatial location sets of the ground truth corresponding semantic instances and the corresponding semantic instances obtained by our method,  $o_{x_i}$  and  $o_{y_j}$  are the spatial locations of the corresponding semantic instances  $I_{x_i}$  and  $I_{y_j}$  belonging to the set  $\Omega$ , and  $1(\cdot)$  is the counting function.  $R_T$  and  $T_T$  represent the ground truth rotation matrix and translation vector contained in KITTI Odometry dataset, respectively.  $\beta$  is the distance threshold and is set to 1m in our method.

RRE and RTE are calculated as follows:

$$E_{RRE} = \sum_{i=1}^3 |angle(i)| \quad (19)$$

$$angle = F(R_T^{-1}R) \quad (20)$$

$$E_{RTE} = \|T_T - T\|_2 \quad (21)$$

where  $R$  and  $T$  are the estimated rotation matrix and the translation vector, the function  $F(\cdot)$  converts the rotation matrix into three Euler angles.

### C. Evaluation Results on the KITTI Odometry Dataset

**Comparison of the inlier ratio.** As can be seen from Table II, our method achieves 54.25% inlier ratio, which is relative higher than others. This is because other methods extract features only relying on the 3D coordinate information and the local context information. Compared with other methods, our method learns the feature from the spatial location

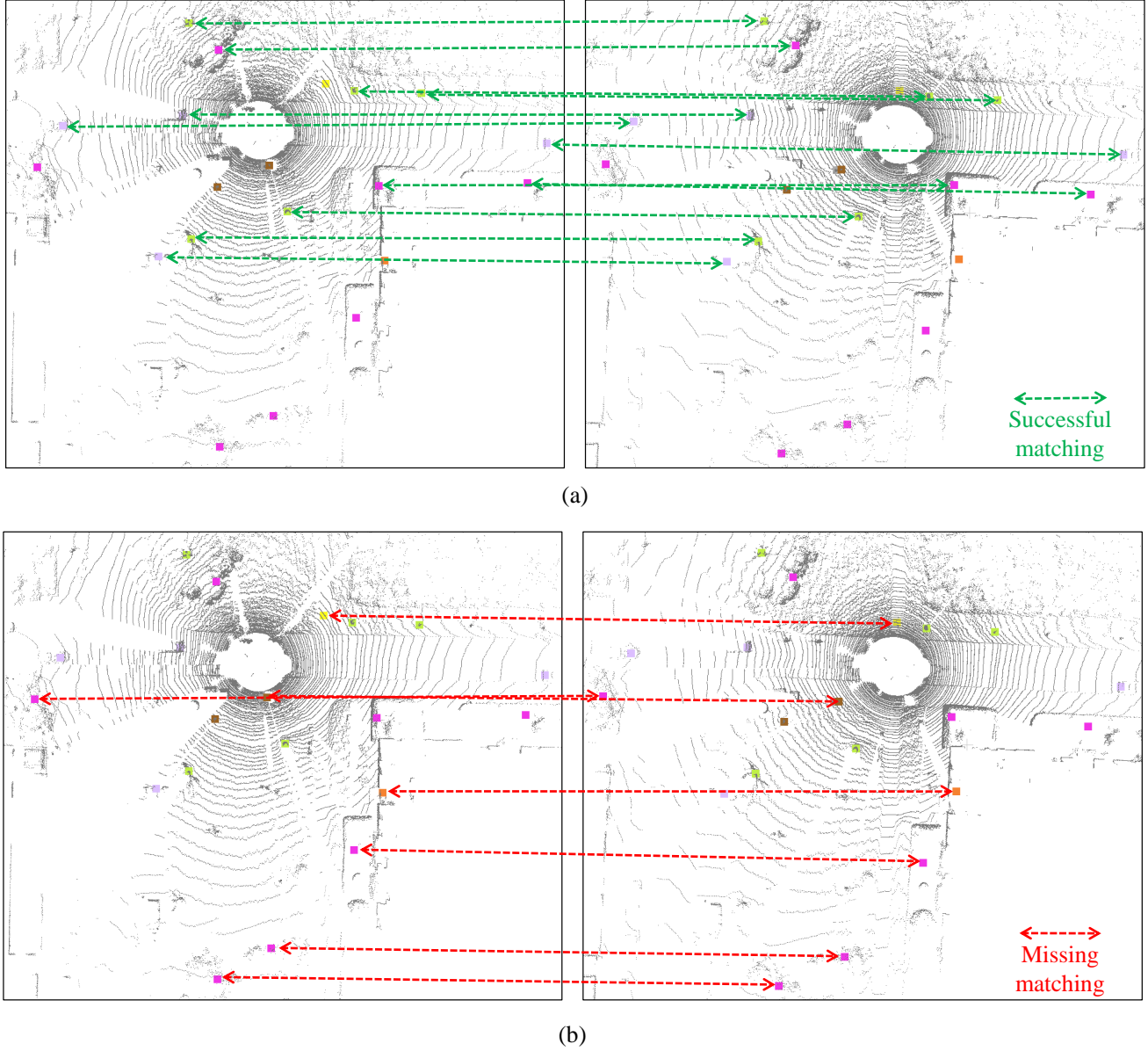


Fig. 7: The visualization of semantic instances matching.

information, semantic categorical information and geometric shape information of semantic instance, and aggregates the context information from two whole scenes. Fig. 7 visualizes the semantic instances matching results. The first row of Fig. 7 shows the semantic instances after pre-processing different colors represent different semantic categorical instances. The second and third rows show the successful matching results and missed matching results. We can observe that all the trunks in the two scenes are correctly matched. This is because the trunks obtained from different angles are basically similar and relatively stable. However, the buildings and sidewalks are relatively difficult to be matched. This is because the spatial location distance of the buildings (or sidewalks) on two scenes are larger than threshold. In these two scenes, there are both successful matching and missed matching instances of

vegetation, and vegetations with relatively dense distribution and close to the scanning center are more likely to find matching instances.

**Comparison of the semantic instance matching accuracy.**

In addition to the inlier ratio, we also adopt the matching accuracy to measure the quality of semantic instance matching, which is expressed as follows:

$$P = \frac{1}{|\Omega|} \sum_{(o_{x_i}, o_{y_j}) \in \Omega} 1(\|(Ro_{x_i} + T) - o_{y_j}\| < \beta) \quad (22)$$

where  $\Omega$  is the spatial location set of matched semantic instances obtained by our method,  $o_{x_i}$  and  $o_{y_j}$  are the spatial locations of corresponding semantic instances  $I_{x_i}$  and  $I_{y_j}$  belonging to  $\Omega$ , and  $1(\cdot)$  is the counting function.  $R_T$  and



TABLE IV: The details of our ablation experiments.

Model	Spatial location	Semantic category	Geometric shape	DGCNN	PointNet	Self-attention	Cross-attention
DSGM-1	✓	✓	✗	✓	✗	✓	✓
DSGM-2	✗	✓	✓	✓	✓	✓	✓
DSGM-3	✓	✓	✓	✓	✓	✗	✗
DSGM-4	✓	✓	✓	✓	✓	✓	✗
ours	✓	✓	✓	✓	✓	✓	✓

TABLE V: The results of ablation experiments.

Methods	RTE(cm)		RRE(°)		Registration	Inlier Ratio (%)	Precision (%)
	AVG	STD	AVG	STD	Success rate (%)		
DSGM-1	6.8	0.018	0.366	0.555	77.04	62.5	82.32
DSGM-2	7.3	0.026	0.25	0.164	87.73	59.63	89.28
DSGM-3	6.6	0.017	0.24	0.138	85.91	48.66	90.7
DSGM-4	6.7	0.019	0.248	0.156	84.32	43.32	90.91
ours	6.6	0.017	0.229	0.143	90.68	54.25	92.97

$T_T$  represent the ground truth rotation matrix and translation vector contained in KITTI Odometry dataset, respectively.  $\beta$  is the distance threshold, and is set to 1m in our method. Through experiments conducted on the KITTI Odometry dataset, our method achieves 92.68% matching accuracy.

**Comparison of the registration performance.** We use the RTE and RRE to evaluate the registration performance of our proposed method. calculate the initial transformation matrix according to the matched semantic instances, and then obtain the final transformation matrix by the ICP algorithm Table III shows the comparison results.

As shown in Table III, in terms of relative translation error, our method can achieve the best performance. The average relative translation error is 6.13cm and the standard deviation of relative translation error is 0.08cm. As for relative rotation error, we can observe that our method can reach the lowest error of 0.22°, but the standard deviation of it is 0.27°, which is higher than the result of D3Feat method of 0.06°. The reasons for the above results are as follows: due to the occlusion of objects in the scene and the change of scanning center, the position of corresponding instances is different, resulting in the fewer matching semantic instances can be extracted and affecting the registration accuracy of the point cloud.

#### D. Ablation Study

In this section, we conduct the ablation experiment to analyze the attributes of the semantic instances and the modules of the network respectively. As for the attributes of the semantic instances, we ignore the geometric shape information and the spatial location information, and call them DSGM-1 and DSGM-2, respectively. As for the modules of the network, we ignore the attention mechanism and the cross-attention, and call them DSGM-3 and DSGM-4, respectively. The details are shown in the following Table IV.

The results of our ablation experiments are shown in Table V. As for ignoring the attributes of semantic instances

(DSGM-1 and DSGM-2), we can see that the geometric shape information and the spatial location information are important to the representation of semantic instances. Although the inlier ratio of DSGM-1 are the best results in DSGM-1, DSGM-2 and DSGM, its success rate is only 77.04%, which is too low for registration. As for ignoring the attention mechanism (DSGM-3 and DSGM-4), we can see that the self-attention and the cross-attention are important to the deep semantic graph matching. If both self-attention and the cross-attention are used, the DSGM can obtain the best experimental results, and the averages of RTE and RRE are 6.6cm and 0.229°, the STD of RTE is 0.017, the success rate is 90.68% and the precision is 92.97%.

## V. CONCLUSION

In this paper, we propose a deep semantic graph matching method for large-scale outdoor point cloud registration. The geometric shape features, semantic categorical features, and spatial distribution features are utilized to describe the semantic instances. The high-dimensional features are then learned and enhanced for each kind of feature through graph convolutional network and enhanced based on self-attention and cross-attention mechanisms. The concatenated features are then fed into the optimal matching layer to obtain semantic instance correspondences. The final geometric transformation matrix is then estimated through a coarse-to-fine registration strategy. The experimental results conducted on the KITTI Odometry dataset demonstrate the feasibility and superiority of the proposed method.

## REFERENCES

- [1] Y. Guo, H. Wang, Q. Hu, H. Liu, L. Liu, and M. Bennamoun, "Deep learning for 3d point clouds: A survey," *IEEE Transactions on Pattern Analysis and Machine Intelligence*, vol. 43, no. 12, pp. 4338–4364, 2021.
- [2] F. Stein and G. Medioni, "Structural indexing: efficient 3-d object recognition," *IEEE Transactions on Pattern Analysis and Machine Intelligence*, vol. 14, no. 2, pp. 125–145, 1992.

- [3] P. Besl and N. D. McKay, "A method for registration of 3-d shapes," *IEEE Transactions on Pattern Analysis and Machine Intelligence*, vol. 14, no. 2, pp. 239–256, 1992.
- [4] A. Johnson and M. Hebert, "Using spin images for efficient object recognition in cluttered 3d scenes," *IEEE Transactions on Pattern Analysis and Machine Intelligence*, vol. 21, no. 5, pp. 433–449, 1999.
- [5] A. Frome, D. Huber, R. Kolluri, T. Bülow, and J. Malik, "Recognizing objects in range data using regional point descriptors," in *Computer Vision-ECCV 2004: 8th European Conference on Computer Vision, Prague, Czech Republic, May 11-14, 2004. Proceedings, Part III* 8. Springer, 2004, pp. 224–237.
- [6] R. B. Rusu, N. Blodow, and M. Beetz, "Fast point feature histograms (fpfh) for 3d registration," in *2009 IEEE International Conference on Robotics and Automation*, 2009, pp. 3212–3217.
- [7] Y. Guo, F. Sohel, M. Bennamoun, M. Lu, and J. Wan, "Rotational projection statistics for 3d local surface description and object recognition," *International journal of computer vision*, vol. 105, pp. 63–86, 2013.
- [8] S. M. Prakhya, B. Liu, and W. Lin, "B-shot: A binary feature descriptor for fast and efficient keypoint matching on 3d point clouds," in *2015 IEEE/RSJ International Conference on Intelligent Robots and Systems (IROS)*, 2015, pp. 1929–1934.
- [9] Z. Dong, B. Yang, Y. Liu, F. Liang, B. Li, and Y. Zang, "A novel binary shape context for 3d local surface description," *ISPRS Journal of Photogrammetry and Remote Sensing*, vol. 130, pp. 431–452, 2017.
- [10] Y. Zhang, C. Li, B. Guo, C. Guo, and S. Zhang, "Kdd: A kernel density based descriptor for 3d point clouds," *Pattern Recognition*, vol. 111, p. 107691, 2021.
- [11] W. Lu, G. Wan, Y. Zhou, X. Fu, P. Yuan, and S. Song, "Deepvcv: An end-to-end deep neural network for point cloud registration," in *2019 IEEE/CVF International Conference on Computer Vision (ICCV)*, 2019, pp. 12–21.
- [12] Y. Wang and J. Solomon, "Deep closest point: Learning representations for point cloud registration," in *2019 IEEE/CVF International Conference on Computer Vision (ICCV)*, 2019, pp. 3522–3531.
- [13] Y. Aoki, H. Goforth, R. A. Srivatsan, and S. Lucey, "Pointnetlk: Robust & efficient point cloud registration using pointnet," in *2019 IEEE/CVF Conference on Computer Vision and Pattern Recognition (CVPR)*, 2019, pp. 7156–7165.
- [14] V. Sarode, X. Li, H. Goforth, Y. Aoki, R. A. Srivatsan, S. Lucey, and H. Choset, "Pernet: Point cloud registration network using pointnet encoding," *arXiv preprint arXiv:1908.07906*, 2019.
- [15] Z. Huang, Z. Gojcic, M. Usvyatsov, A. Wieser, and K. Schindler, "Predator: Registration of 3d point clouds with low overlap," in *2021 IEEE/CVF Conference on Computer Vision and Pattern Recognition (CVPR)*, 2021, pp. 4265–4274.
- [16] Z. Qin, H. Yu, C. Wang, Y. Guo, Y. Peng, and K. Xu, "Geometric transformer for fast and robust point cloud registration," in *2022 IEEE/CVF Conference on Computer Vision and Pattern Recognition (CVPR)*, 2022, pp. 11 133–11 142.
- [17] W. Shi and R. Rajkumar, "Point-gnn: Graph neural network for 3d object detection in a point cloud," in *2020 IEEE/CVF Conference on Computer Vision and Pattern Recognition (CVPR)*, 2020, pp. 1708–1716.
- [18] C. R. Qi, L. Yi, H. Su, and L. J. Guibas, "Pointnet++: Deep hierarchical feature learning on point sets in a metric space," *Advances in neural information processing systems*, vol. 30, 2017.
- [19] F. Groh, P. Wieschollek, and H. P. Lensch, "Flex-convolution: Million-scale point-cloud learning beyond grid-worlds," in *Asian Conference on Computer Vision*. Springer, 2018, pp. 105–122.
- [20] Y. Zhong, "Intrinsic shape signatures: A shape descriptor for 3d object recognition," in *2009 IEEE 12th international conference on computer vision workshops, ICCV Workshops*. IEEE, 2009, pp. 689–696.
- [21] A. Mian, M. Bennamoun, and R. Owens, "On the repeatability and quality of keypoints for local feature-based 3d object retrieval from cluttered scenes," *International Journal of Computer Vision*, vol. 89, pp. 348–361, 2010.
- [22] I. Sipiran and B. Bustos, "Harris 3d: a robust extension of the harris operator for interest point detection on 3d meshes," *The Visual Computer*, vol. 27, pp. 963–976, 2011.
- [23] A. Du, X. Huang, J. Zhang, L. Yao, and Q. Wu, "Kpsnet: Keypoint detection and feature extraction for point cloud registration," in *2019 IEEE International Conference on Image Processing (ICIP)*. IEEE, 2019, pp. 2576–2580.
- [24] Y. Wang and J. M. Solomon, "Prnet: Self-supervised learning for partial-to-partial registration," *Advances in neural information processing systems*, vol. 32, 2019.
- [25] X. Bai, Z. Luo, L. Zhou, H. Fu, L. Quan, and C.-L. Tai, "D3feat: Joint learning of dense detection and description of 3d local features," in *2020 IEEE/CVF Conference on Computer Vision and Pattern Recognition (CVPR)*, 2020, pp. 6358–6366.
- [26] S. Liu, T. Wang, Y. Zhang, R. Zhou, C. Dai, Y. Zhang, H. Lei, and H. Wang, "Rethinking of learning-based 3d keypoints detection for large-scale point clouds registration," *International Journal of Applied Earth Observation and Geoinformation*, vol. 112, p. 102944, 2022.
- [27] X. Kong, X. Yang, G. Zhai, X. Zhao, X. Zeng, M. Wang, Y. Liu, W. Li, and F. Wen, "Semantic graph based place recognition for 3d point clouds," in *2020 IEEE/RSJ International Conference on Intelligent Robots and Systems (IROS)*, 2020, pp. 8216–8223.
- [28] Y. Zhu, Y. Ma, L. Chen, C. Liu, M. Ye, and L. Li, "Gosmatch: Graph-of-semantics matching for detecting loop closures in 3d lidar data," in *2020 IEEE/RSJ International Conference on Intelligent Robots and Systems (IROS)*. IEEE, 2020, pp. 5151–5157.
- [29] J. Li, S. Huang, H. Cui, Y. Ma, and X. Chen, "Automatic point cloud registration for large outdoor scenes using a priori semantic information," *Remote Sensing*, vol. 13, no. 17, p. 3474, 2021.
- [30] M. A. Fischler and R. C. Bolles, "Random sample consensus: a paradigm for model fitting with applications to image analysis and automated cartography," *Communications of the ACM*, vol. 24, no. 6, pp. 381–395, 1981.
- [31] D. Aiger, N. J. Mitra, and D. Cohen-Or, "4-points congruent sets for robust pairwise surface registration," in *ACM SIGGRAPH 2008 papers*, 2008, pp. 1–10.
- [32] N. Mellado, D. Aiger, and N. J. Mitra, "Super 4pcs fast global point cloud registration via smart indexing," in *Computer graphics forum*, vol. 33, no. 5. Wiley Online Library, 2014, pp. 205–215.
- [33] R. Q. Charles, H. Su, M. Kaichun, and L. J. Guibas, "Pointnet: Deep learning on point sets for 3d classification and segmentation," in *2017 IEEE Conference on Computer Vision and Pattern Recognition (CVPR)*, 2017, pp. 77–85.
- [34] A. Kurobe, Y. Sekikawa, K. Ishikawa, and H. Saito, "Corsnet: 3d point cloud registration by deep neural network," *IEEE Robotics and Automation Letters*, vol. 5, no. 3, pp. 3960–3966, 2020.
- [35] H. Xu, S. Liu, G. Wang, G. Liu, and B. Zeng, "Omnet: Learning overlapping mask for partial-to-partial point cloud registration," in *Proceedings of the IEEE/CVF International Conference on Computer Vision*, 2021, pp. 3132–3141.
- [36] R. Zhou, X. Li, and W. Jiang, "Scanet: a spatial and channel attention based network for partial-to-partial point cloud registration," *Pattern Recognition Letters*, vol. 151, pp. 120–126, 2021.
- [37] D. Streiff, L. Bernreiter, F. Tschopp, M. Fehr, and R. Siegwart, "3d3l: Deep learned 3d keypoint detection and description for lidars," in *2021 IEEE International Conference on Robotics and Automation (ICRA)*, 2021, pp. 13 064–13 070.
- [38] O. Duchenne, A. Joulain, and J. Ponce, "A graph-matching kernel for object categorization," in *2011 International Conference on Computer Vision*, 2011, pp. 1792–1799.
- [39] N. Ufer and B. Ommer, "Deep semantic feature matching," in *Proceedings of the IEEE conference on computer vision and pattern recognition*, 2017, pp. 6914–6923.
- [40] F. Zhou and F. De la Torre, "Factorized graph matching," *IEEE Transactions on Pattern Analysis and Machine Intelligence*, vol. 38, no. 9, pp. 1774–1789, 2016.
- [41] M. Cho, K. Alahari, and J. Ponce, "Learning graphs to match," in *2013 IEEE International Conference on Computer Vision*, 2013, pp. 25–32.
- [42] W.-Z. Nie, A.-A. Liu, Y. Gao, and Y.-T. Su, "Hyper-clique graph matching and applications," *IEEE Transactions on Circuits and Systems for Video Technology*, vol. 29, no. 6, pp. 1619–1630, 2019.
- [43] R. Zhang and W. Wang, "Second- and high-order graph matching for correspondence problems," *IEEE Transactions on Circuits and Systems for Video Technology*, vol. 28, no. 10, pp. 2978–2992, 2018.
- [44] A. Zanfir and C. Sminchisescu, "Deep learning of graph matching," in *2018 IEEE/CVF Conference on Computer Vision and Pattern Recognition*, 2018, pp. 2684–2693.
- [45] R. Wang, J. Yan, and X. Yang, "Learning combinatorial embedding networks for deep graph matching," in *2019 IEEE/CVF International Conference on Computer Vision (ICCV)*, 2019, pp. 3056–3065.
- [46] Y. Wang, Y. Sun, Z. Liu, S. E. Sarma, M. M. Bronstein, and J. M. Solomon, "Dynamic graph cnn for learning on point clouds," *ACM Transactions on Graphics (tog)*, vol. 38, no. 5, pp. 1–12, 2019.